CONF-8505112--7

BNL 38296

DESCRIPTION OF AN XRF SYSTEM FOR MULTIELEMENTAL ANALYSIS

L. Wielopolski*

R. Zhang

S.H. Cohn

BNL--38296

DE86 013912

Brookhaven National Laboratory

Medical Research Center

Upton, LI, New York 11973

Index Entry: XRF, multielemental analysis, orthogonal configuration, spatial uniformity.

This research was carried out in part under contract no. De-AC-02-75CH00016 with the United States Department of Energy.

ABSTRACT

An X-ray fluorescence (XRF) system which uses radioisotopes in an orthogonal configuration between the source, sample, and detector is described. The advantage of such a system is that for large (bulk) samples or for in vivo measurements the background due to Compton scattering in the sample is minimized. High reproducibility for nonuniform samples is obtained by reducing the sample size and thus the effects of non-uniformity in the spatial response of such a system. Germane to any accurate analytical method is the use of proper mathematical algorithms for data evaluation. The problem is acute, in particular, when photopeaks with low counting statistics are to be analyzed. In the case of a single photopeak on flat, background optimal energy window size, which maximizes the signal-to-noise ratio, for trapezoidal intergration is described. The sensitivity and minimum detection limit at different energies together with background considerations are discussed.

INTRODUCTION

X-ray spectroscopy dates back to around 1910 when Barkla (1) obtained the first positive evidence of characteristic x-ray emission spectra. Three years later, Moseley (2) established the relationship between frequency (energy) and atomic number. However, only in the last three decades, with the invention of lithium-drifted silicon and germanium solid state detectors (3), has x-ray fluorescence (XRF) spectrometry been established as a valid and reliable analytical tool.

The main advantages of the XRF technique are its very wide dynamic range in elemental concentration that can be measured (from 100% down to trace quantities in the parts-per-billion (ppb) range), its ability to perform nondestructive, multielemental analysis, and the fact that it requires little to no sample preparation. The analyzed samples can be either solid, liquid, or gaseous. The spectral distribution of x-rays is almost unambiguous. The few cases where ambiguity does occur are well known and can be resolved either analytically or by the use of different characteristic lines. Finally, all the elements above boron are amenable to analysis by XRF regardless of their chemical state (4-6).

Most of the high-throughput, sophisticated, XRF systems which have been developed use x-ray machines or alternative powerful sources of radiation to excite the sample. In some cases, however, XRF systems with low-throughput can be justified. Characteristics and design parameters of such a system, in which radioisotopes are used as an excitation source in orthogonal configuration, are described. This system is capable of analyzing trace elements in the sub-ppm level and requires tens of nanograms of material for the analysis.

DESIGN CONSIDERATIONS OF AN XRF SYSTEM

The main considerations in the development of an XRF system are a) mode of excitation, b) source-sample-detector configuration, c) detection system, d) line intensity evaluation, e) suitable calibration procedure. Some of these considerations depend upon the type of samples to be analyzed.

A low throughput system can be designed, with low cost and minimum maintenance requirements, using radioisotopes as the source of radiation to excite the sample. In this case it is important to choose a radioisotope with the energy best suited to excite the elements of interest in the sample. Since the characteristic x-ray yield is governed by a) photoelectric cross section (τ), b) the jump ratio (1-j) (i.e., the probability that the vacancy will be created in either the K or the L shell, c) fluorescence yield (ω) probability that x-ray emission occurs, and d) detection efficiency (η), the x-ray yield (Y) can be written as

$$Y = c\tau\omega\,(1-j)\,\eta, \qquad (1)$$

where c is a proportionality constant which includes the solid angles, the source intensity, and the elemental abundance in the sample. The calculated yields for a 3-mm-thick Si(Li) detector with a 1-mil-thick beryllium entrance window, and assuming c equals 1, are shown in Fig. 1. The yields have been calculated for K x-rays induced by 20- and 60-keV incident excitation radiation and for L x-rays at 20 keV. It is seen that all the elements in the periodic table can be measured, except the low Z elements which require windowless detectors. Furthermore, it is also evident that excitation energies closer to the absorption edge provide higher x-ray yields.

The source-sample-detector configuration is possible in a variety of geometries such as annular source, central source, and side source. The side source configuration, chosen in the present work, offers a large selection of point sources available commercially. But more important, when bulk samples are analyzed, or in in vivo measurements, positioning the source at 90° with regard to the detector-sample axis provides minimum scattered radiation, thus reducing the count rate and the background in the detector. This follows directly from the differential scattering cross section ($d\sigma_e/d\Omega$) as expressed by the Klein-Nishina formula (7)

$$d\sigma_e/d\Omega = (r^2/2)\ (E'/E)^2\ (E'/E + E/E' - \sin^2\theta), \qquad (2)$$

where r_o is the classical electron radius, E and E' are the photon energies before and after scattering, respectively, and θ is the scattering angle. Differential scattering probability as a function of the scattering angle θ is shown at different energies E in Fig. 2.

In the side source configuration, where the source-sample-detector path is in a horizontal plane, the response from a thin sample located perpendicular to the radiation path is not uniform. The spatial response of a 1x1-mm thin copper foil moved in the x and y directions, as shown in Fig. 3, resulted in the intensity distribution of Cu x-rays shown in Figs. 4-6. The asymmetry in the x direction depends on the diameter of the source collimator. For example, in Fig. 4 where the diameter is larger than that in Fig. 6, two different sources were used. The response along the y axis, Fig. 5, is symmetric.

The nonuniform spatial response requires that the sample size be maintained constant during sample preparation. This is demonstrated by evaporating different volumes of lead solution in a center of Formvar film and monitoring the lead x-ray yield. The x-ray yield per unit volume (10 µl) decreased while the dry sample diameter increased when the sample volume was increased (Fig. 7a). However, when the sample was prepared by drying constant volumes consecutively, thus maintaining the dry sample diameter constant, the yield per unit volume remained fairly constant (Fig. 7b). The reproducibility of the system for a-6mm dry sample size is about 2%.

The analytical method used to evaluate the peak intensities depends on the degree of spectral complexity. In the case of intense and clearly separated peaks, almost any method is equally valid and should yield identical results. For complex spectra, the least-squares method (8,9) is the most appropriate one. However, when peaks with low counting statistics are measured, hand analysis and trapezoidal integration of the background are about the only available methods (10). In this method, in order to obtain the best signal-to-noise ratio (SN), the optimum window width over which the peak is integrated is about 1.4σ or 0.6 FWHM, where σ is the standard deviation of the Gaussian peak and FWHM is the full width at half maximum of the peak. The SN is defined as the ratio of the net number of counts in the peak to the square root of the number of counts in the background. The behavior of SN as a function of the window width is shown in Fig. 8. For low-intensity peaks the relative error is inversely proportional to SN. The drawback in using the optimum size window is that the results are sensitive to electronic instabilities.

Reduction of background in XRF spectroscopy is important in order to improve the signal to noise ratio and to decrease the minimum detectable limit of the system. For large samples the background is reduced by the orthogonal configuration of the source-sample-detector geometry. For thin samples, the background may be reduced by decreasing the mass of the backing material which supports the sample. The background conditions for backing materials with different surface density are summarized in Table I. Since the backing materials are low Z, Compton Rayleigh ratio (Nc/Nr) increases with the increase in surface density. Additional background, from radiation scattering in the air, can be reduced significantly by positioning the head of the detector in a vacuum chamber. The minimum detectable limits for a few elements, which were dried separately on a Formvar film, are summarized in Table II. The minimum detection limits are quoted in ng in 100 µl sample. Since counting rates were significantly below the counting capability of the system, an increase in the source intensity and the counting time would reduce the MDL values even further. Improvement in MDL by a factor of 10 is conceivable. Use of lower excitation energy (^{55}Fe source Mn x-rays) will also further improve the measurements for low Z elements. An XRF spectrum obtained with the present system is shown in Ref. 13.

SUMMARY

Many x-ray spectrometers are currently being used for routine qualitative and quantitative analysis. Most of the systems use powerful x-ray machines. However, when the speed of analysis is not of primary concern, systems employing radioisotope sources can be used very effectively.

There are many factors which influence the design of an XRF system. The most important factors and their optimal settings were discussed earlier. The capability of the present system to analyze trace elements is demonstrated in Table II, where sensitivities in the sub-ppm region can be attained. Applications of the present XRF system for in vitro and in vivo analyses are summarized in refs. 11 to 13.

REFERENCES

1. C.G. Barkla, The Spectra of the fluorescent Rontgen Radiations. Phil. Mag., 22 (1911) 396.
2. H.G.J. Moseley, High frequency spectra of the elements, Phil. Mag., 27 (1914) 703.
3. H.R. Bowman, E.K. Hyde, S.G. Thompson, and R.C. Jared, Application of high-resolution semiconductor detectors in x-ray emmission spectrography, Science, 151 (1966) 562.
4. L. Kaufman and D.C. Price eds., Medical Applications of Fluorescent Excitation Analysis, CRC Press, Inc. 1979.
5. R. Jenkins, R.W. Gould, D. Gedcke, Quantitative X-Ray Spectrometry, Marcel Dekker, Inc. 1981.
6. R. Cesareo, X-Ray Fluorescence (XRF and PIXE) in Medicine, Field Educational Italia Acta Medica, Rome (1982).
7. R.D. Evens, Compton Effect, S. Flugge ed. Encyclopedia of Physics, Springer-Verlag, Berlin Gottingen Heidelberg XXXIV (1958).
8. R.P. Gardner, L. Wielopolski, K. Verghese, Applications of selected mathematical techniques to energy dispersive x-ray fluorescence analysis, At. Energy Rev., 15 (1977) 701-756.
9. L. Wielopolski, Application of Si(Li) detector response function for the analysis of a tungsten library standard, Nucl. Instr. Methods, 190 (1981) 177-180.
10. G.W. Phillips, Filtering peaks with very low statistics, Nucl. Instr. Methods 153 (1978) 449-455.
11. L. Wielopolski, D. Vartsky, S.H. Cohn, In vivo elemental analysis utilizing XRF techniques, Neurotoxicology 4 (1983) 173-176.

12. L. Wielopolski, J.D.B. Featherstone, S.H. Cohn, Measurement of Ca, Zn, and Sr in enamel of human teeth by XRF, J.R. Vogt ed., Nuclear Methods In Environmental and Energy Research Conf. - 840408 (1984) 742-750.

13. L. Wielopolski, R. Zhang, M.J. Clarke, S.H. Cohn, Determination of Ruthenium on DNA by XRF, Present issue.

Table I

Background distribution (number of counts per hour) integrated over 300 eV (10 channels) at the position of different elements.

	Surface density (mg/cm^2)	Ar	Ca	Cu	Zn	Pb_α	Pb_β	Br	Sr	Compton	Rayleigh	Nc/Nr
No Source	-	47	40	26	23	21	18	19	19	16	17	1
Only source	-	1006	341	429	390	373	371	351	332	3382	1410	2.4
Formvar foil	0.025	1020	387	411	410	384	370	365	328	3330	1378	2.4
Thin Parafilm	0.306	973	590	420	406	382	367	375	330	4000	1437	2.8
Normal Parafilm	11.580	1409	788	610	610	593	617	630	590	35153	6048	5.8

Table II

MDL in 100 μL samples, attained in 1 hr counting time with a 100-mCi ^{125}I source

Element	Z	MDL* (ng)
Ca	20	1300
Cu	29	43
Zn	30	40
Sr	38	10
Ru	44	10
Cd	48	30
Pb**	82	270

* MDL is defined as three times the square root of the background.

** Lead L x-rays.

FIGURE CAPTIONS

Fig. 1 Relative x-ray fluorescence yield.

Fig. 2 Differential Compton scattering probability as a function of the scattering angle at different incident energies.

Fig. 3 The geometrical setup for mapping the spatial response.

Fig. 4 The spatial response in x direction from a ^{109}Cd source.

Fig. 5 The spatial response in y direction from a ^{109}Cd source.

Fig. 6 The spatial response in x direction from a ^{125}I source held in a collimator with a smaller diameter than the ^{109}Cd source.

Fig. 7 The lead x-ray yield per unit volume versus sample volume: a) dry sample diameter increases b) consecutive drying of constant volume.

Fig. 8 Signal-to-noise ratio versus the width of the integration interval.

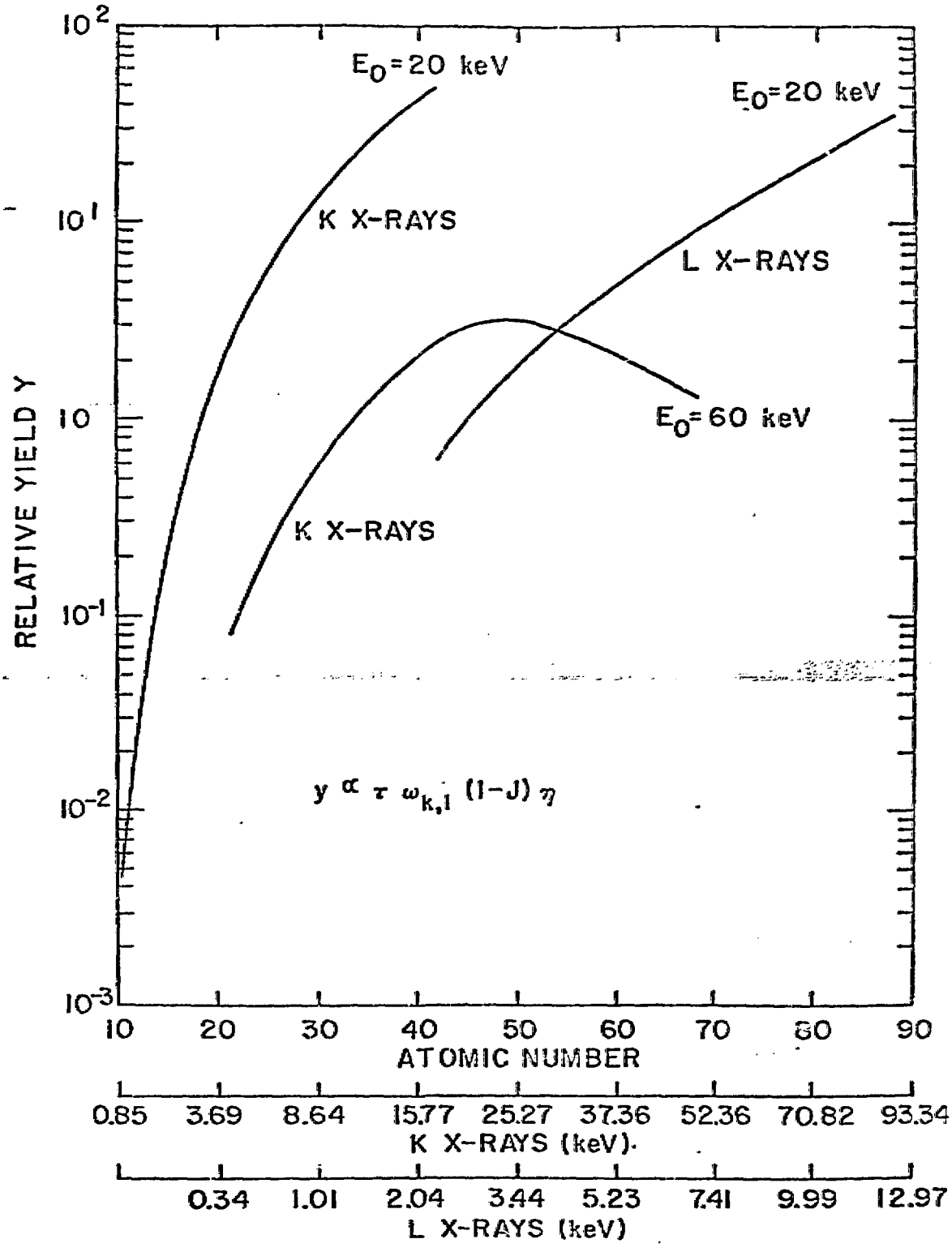

Fig. 1 Relative x-ray fluorescence yield.

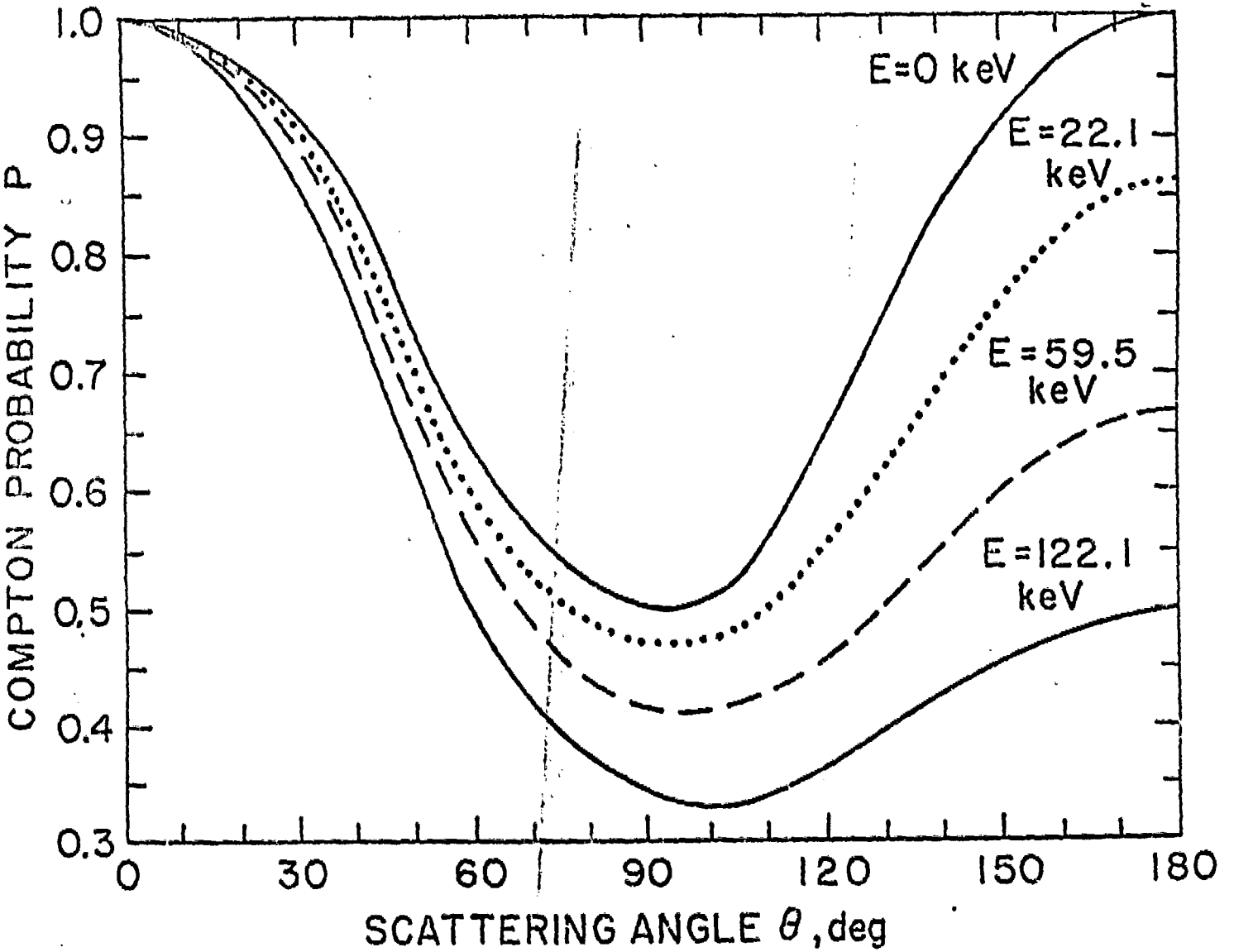

Fig. 2 Differential Compton scattering probability as a function of the scattering angle at different emitted energies.

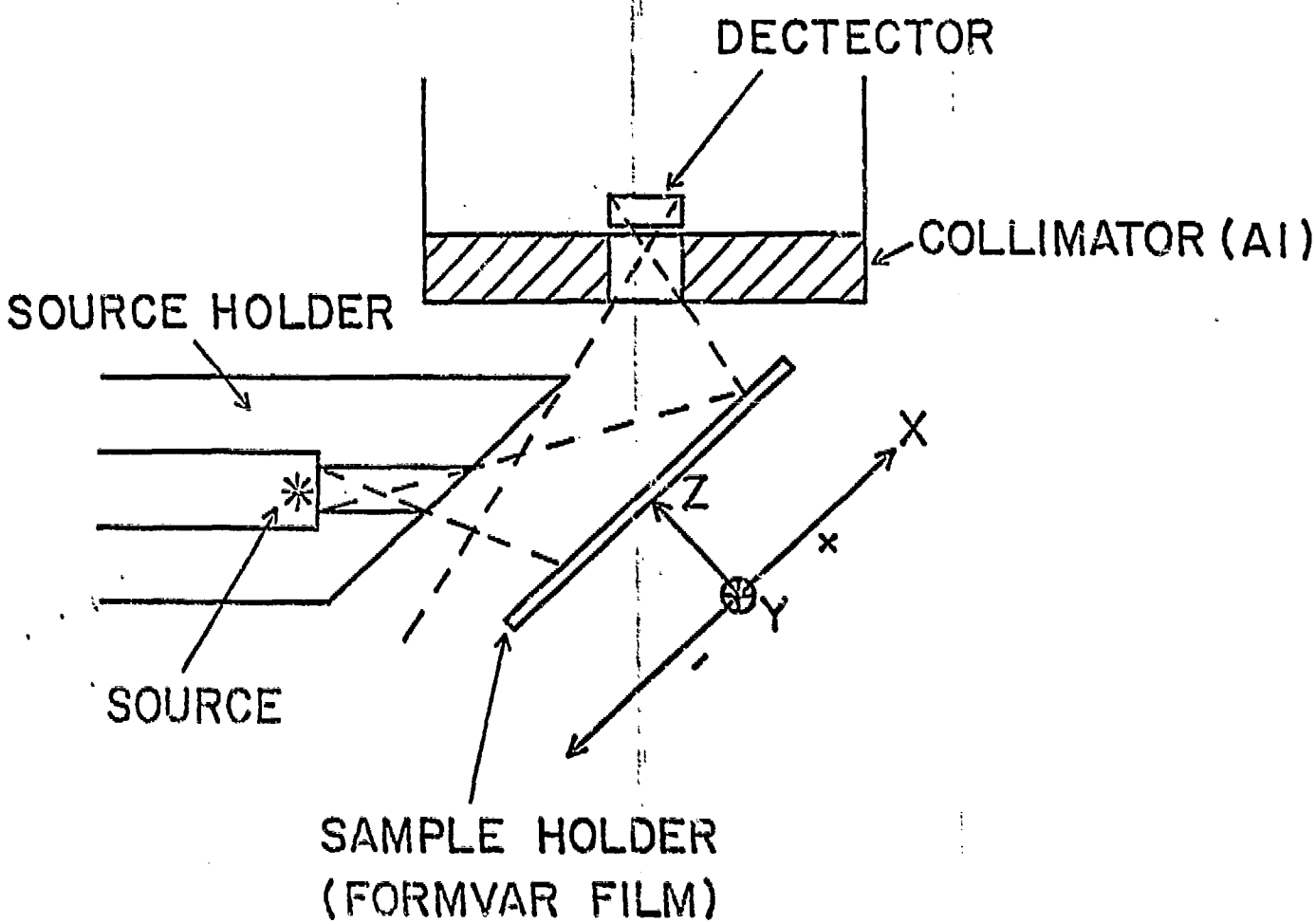

Fig. 3 The geometrical setup for mapping the spatial response.

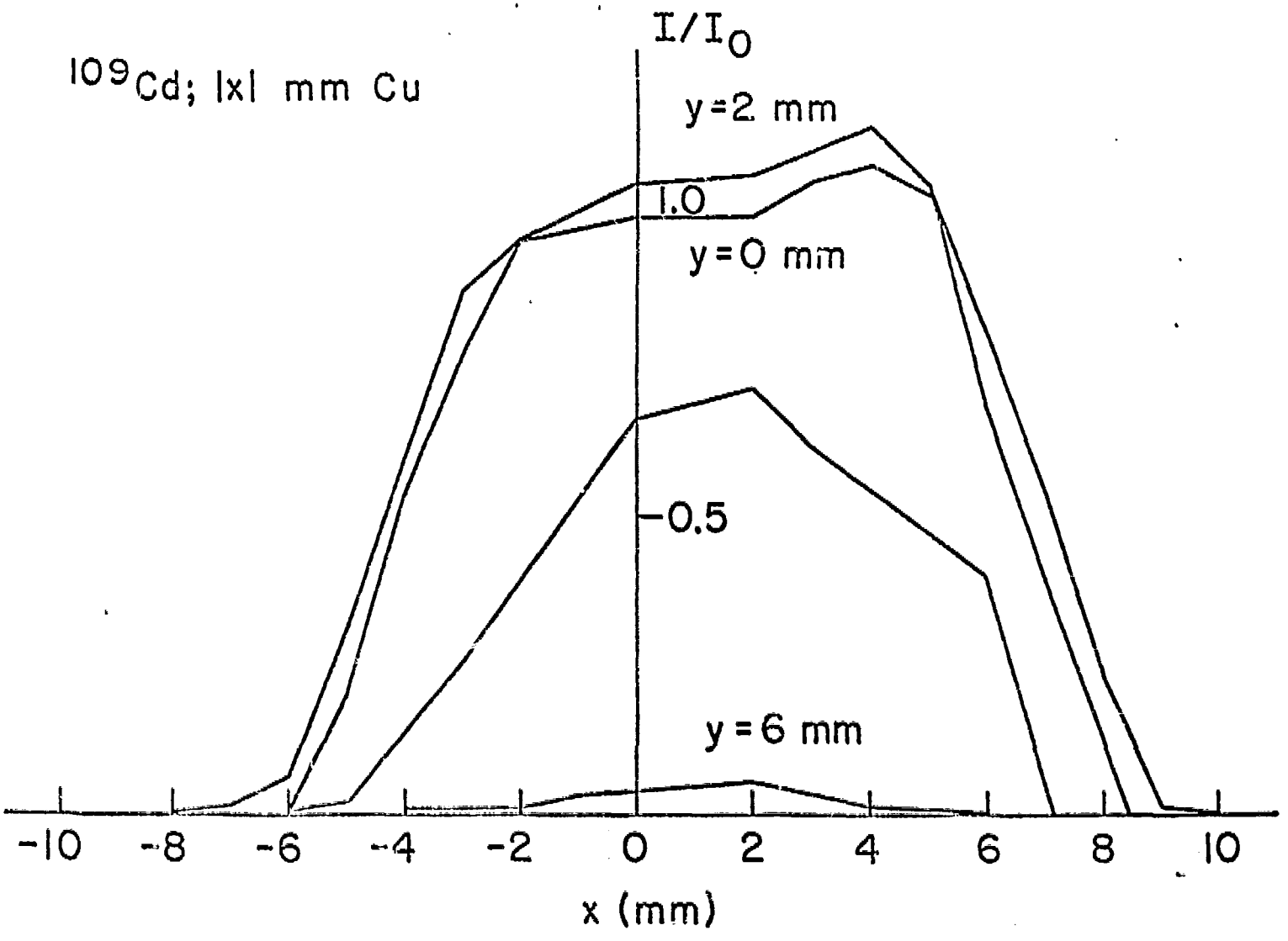

Fig. 4 The spatial response in x direction

from a ^{109}Cd source

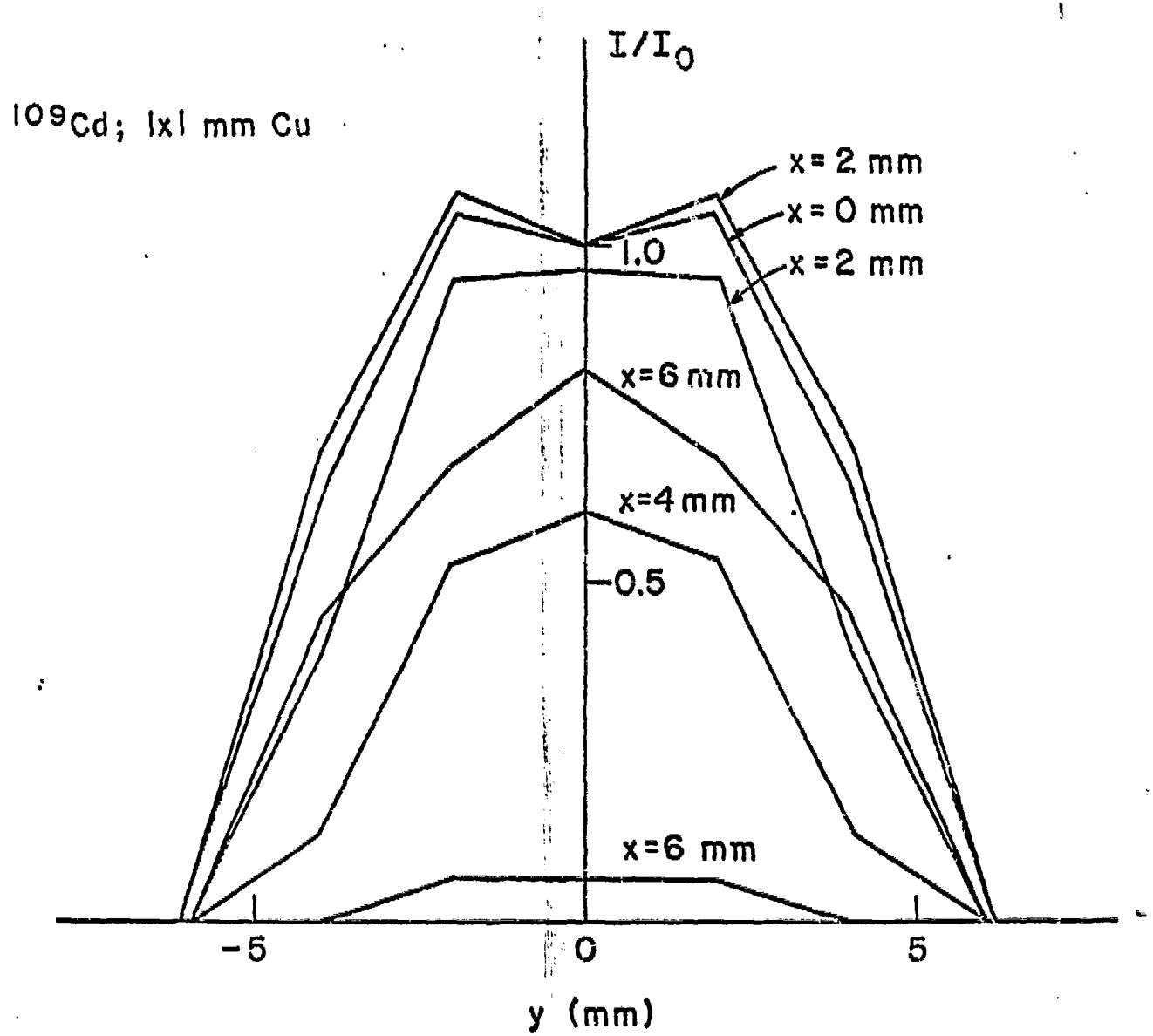

Fig. 5 The spatial response in y direction from a ^{109}Cd source.

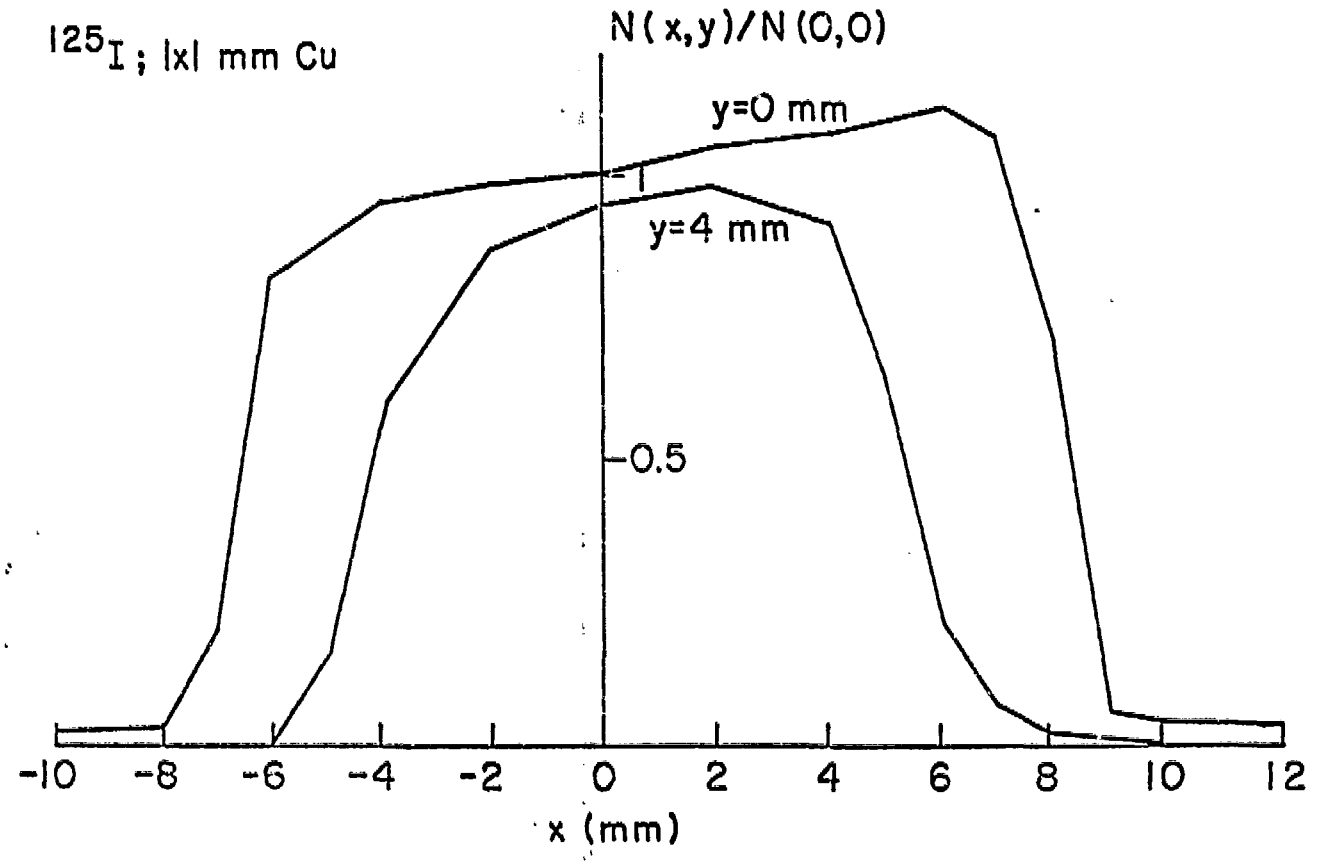

Fig. 6 The spatial response in x direction from a ^{125}I source held in a collimator with a

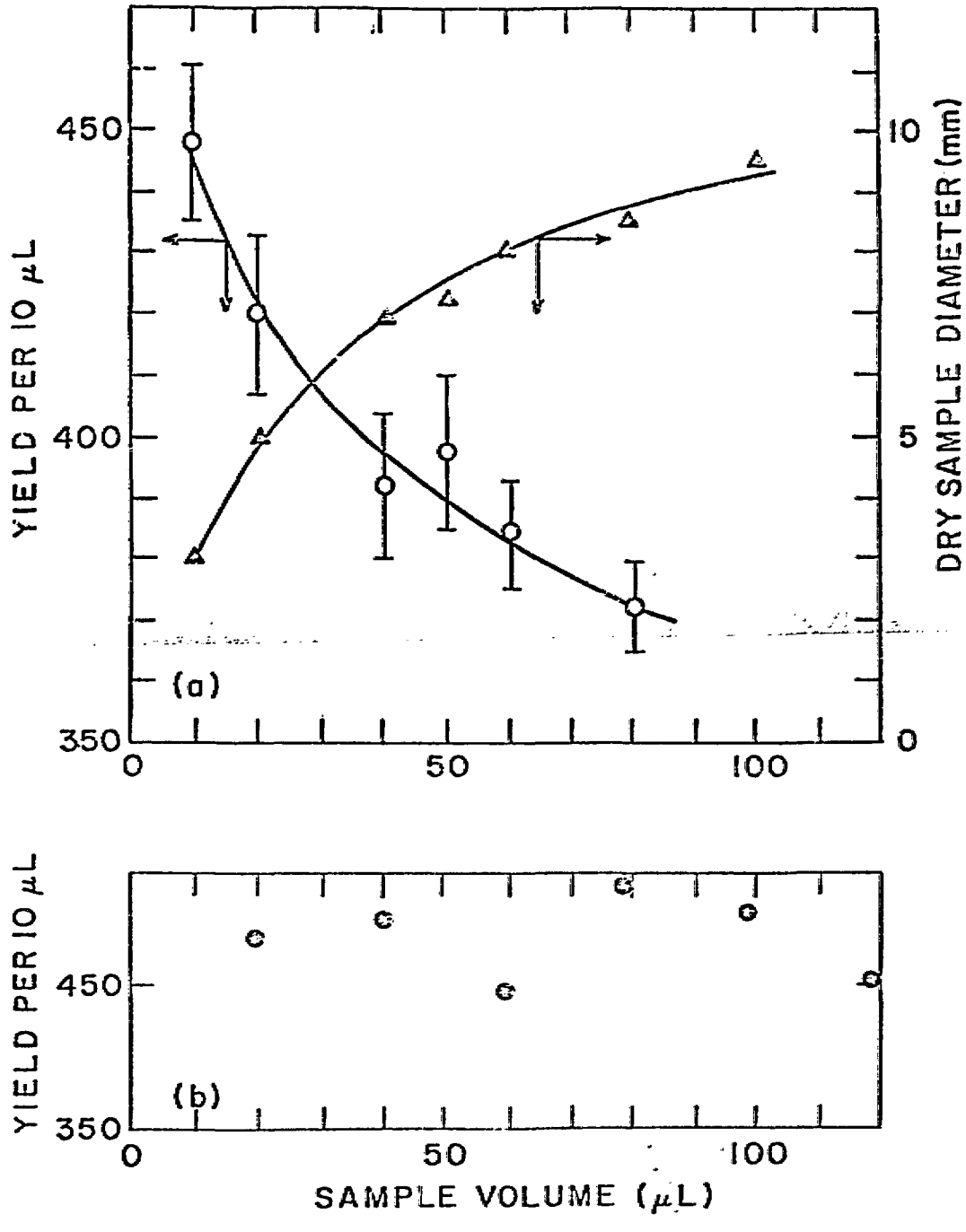

Fig. 7 The lead x-ray yield per unit volume versus sample volume:
a) dry sample diameter increases
b) consecutive drying of constant volume.

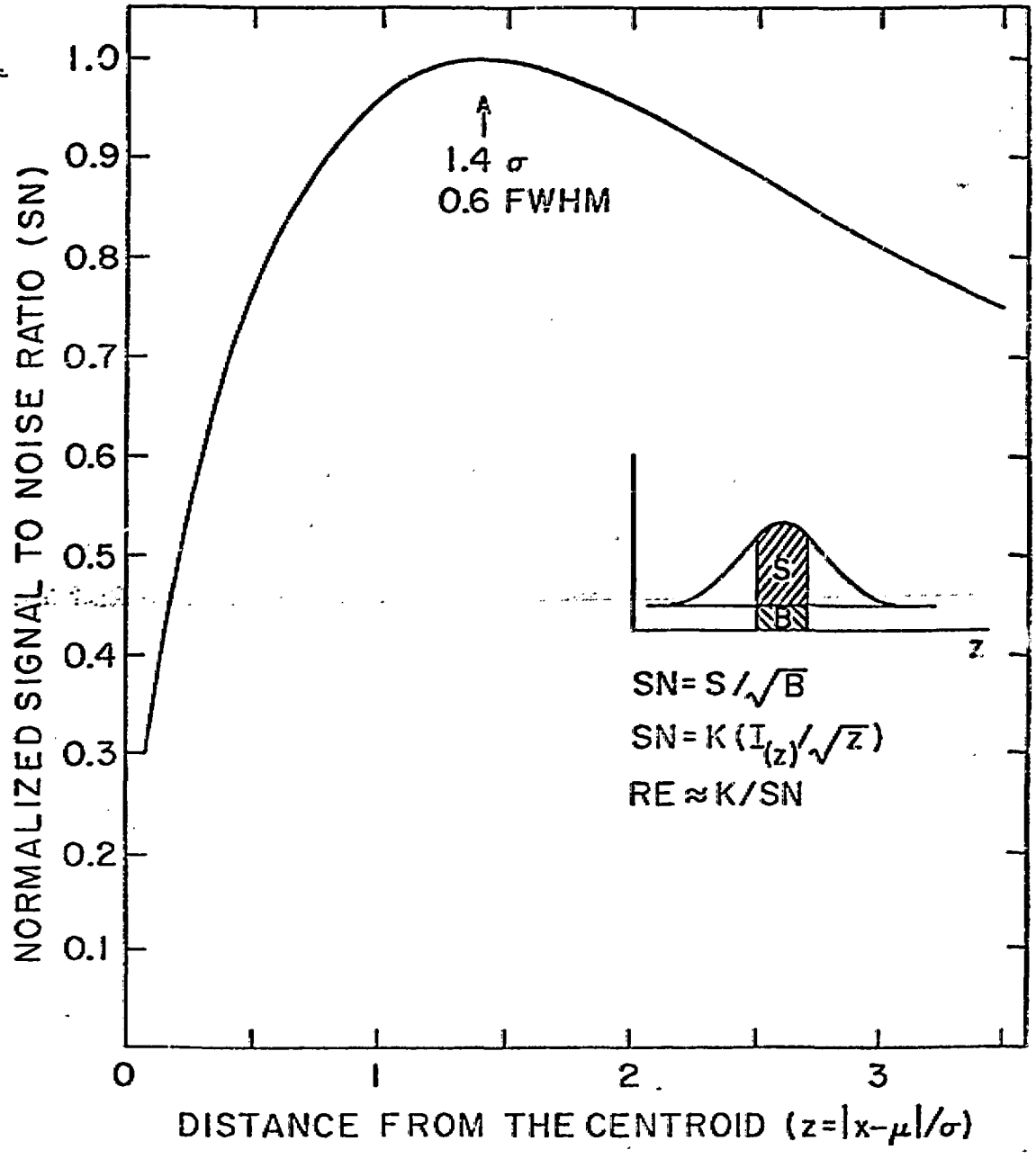

Fig. 8 Signal-to-noise- ratio versus the width of the integration interval.

DISCLAIMER